

Available online at www.sciencedirect.com**SciVerse ScienceDirect**

Procedia Environmental Sciences 19 (2013) 47 – 56

Procedia

Environmental Sciences

Four Decades of Progress in Monitoring and Modeling of Processes in the Soil-Plant-Atmosphere System: Applications and Challenges

Using a diagnostic soil-plant-atmosphere model for monitoring drought at field to continental scales

Martha C. Anderson^{a*}, Carmelo Cammalleri^a, Christopher R. Hain^b, Jason Otkin^c, Xiwu Zhan^d, William Kustas^a

^aUSDA-ARS Hydrology and Remote Sensing Lab, 10300 Baltimore Ave, Beltsville, MD 20705, USA

^bEarth System Science Interdisciplinary Center, University of Maryland, College Park, MD USA

Abstract

Drought assessment is a complex undertaking, requiring monitoring of deficiencies in multiple components of the hydrologic budget. Precipitation anomalies reflect variability in water supply to the land surface, while soil moisture, groundwater and surface water anomalies reflect deficiencies in moisture storage. In contrast, evapotranspiration (ET) anomalies provide unique yet complementary information, reflecting variations in actual water use by crops – a useful diagnostic of vegetation health. Here we describe a remotely sensed Evaporative Stress Index (ESI) based on anomalies in actual-to-reference ET ratio. Actual ET is retrieved from thermal remote sensing data using a diagnostic soil-plant-atmosphere modeling system forced by measurements of morning land-surface temperature (LST) rise from geostationary satellites. In comparison with vegetation indices, LST is a relatively fast-response variable, with the potential for providing early warning of crop stress reflected in increasing canopy temperatures. Spatiotemporal patterns in ESI have been compared with patterns in the U.S. Drought Monitor and in standard precipitation-based indices, demonstrating reasonable agreement. However, because ESI does not use precipitation as an input, it provides an independent assessment of evolving drought conditions, and is more portable to data-sparse parts of the world lacking dense rain-gauge and Doppler radar networks. Integrating LST information from geostationary and polar orbiting systems through data fusion, the ESI has unique potential for sensing moisture stress at field scale, with potential benefits to yield estimation and loss compensation efforts. The ESI is routinely produced over the continental U.S. using data from the Geostationary Operational Environmental Satellites, with expansion to North and South America underway. In addition drought and ET monitoring applications are being developed over Africa and Europe using land-surface products from the Meteosat Second Generation (MSG) platform.

© 2013 The Authors. Published by Elsevier B.V. Open access under [CC BY-NC-ND license](https://creativecommons.org/licenses/by-nc-nd/4.0/).

Selection and/or peer-review under responsibility of the Scientific Committee of the conference

* Corresponding author. Tel.: 301-504-6616; fax: 301-504-8931.

E-mail address: martha.anderson@ars.usda.gov.

Keywords: Evapotranspiration, drought, thermal remote sensing, energy balance

1. Introduction

There is a need for robust information about vegetation health and drought impacts over a broad range in spatial scales in support of applications from field management to monitoring for global food security. Diagnostic soil-plant-atmosphere models constrained by remote sensing can play a critical role in these operational efforts. The agronomic and micrometeorological information encoded in these models adds interpretive value to standard drought indicators, which are based primarily on precipitation anomalies. These models provide a means to diagnose actual stress experienced by crops and natural vegetation, rather than potential for stress as implied by moisture supply deficits alone.

A key input to diagnostic models of land-surface water use and energy balance is the land-surface temperature (LST), which can be retrieved from satellite or airborne observations collected in the thermal infrared (TIR) wavebands. LST captures elevations in stressed canopy and dry soil temperatures that convey useful information regarding surface moisture status to land-surface modeling systems (LSMs). Prognostic LSMs based on water balance require a significant amount of additional information (e.g., rainfall and moisture inputs from irrigation or groundwater, soil texture, plant rooting depth and stress response functions) to obtain similar assessments of moisture status and stress. Furthermore, LST data can be collected over range in scales unattainable by prognostic LSMs, which are principally constrained by the resolution of the rainfall data. An optimal drought and crop monitoring system might combine both prognostic and diagnostic elements to provide the most reliable signals, particularly under conditions of rapid stress onset.

Here describe the development and assessment of an Evaporative Stress Index (ESI) at continental scales, reflecting anomalies in evapotranspiration (ET) retrieved using thermal band imagery from geostationary satellite platforms. We also outline plans for implementation at field scales using data fusion techniques, combining LST data collected at higher spatial resolution from polar orbiting systems like Landsat. These multi-scale assessments of anomalous crop water use have potential utility for regional drought and crop condition monitoring as well as for water management and yield estimation.

2. ET Modeling framework

2.1. ALEXI/DisALEXI

The ALEXI/DisALEXI surface energy balance model [1,2] (Fig. 1) was specifically designed to minimize the need for ancillary meteorological data while maintaining a physically realistic representation of land-atmosphere exchange over a wide range in vegetation cover conditions. It is one of few diagnostic land-surface models designed explicitly to exploit the high temporal resolution afforded by geostationary satellites.

Surface energy balance models estimate ET by partitioning the energy available at the land surface ($RN - G$, where RN is net radiation and G is the soil heat conduction flux, in Wm^{-2}) into turbulent fluxes of sensible and latent heating (H and λE , respectively, Wm^{-2}):

$$RN - G = H + \lambda E \quad (1)$$

where λ is the latent heat of vaporization ($J kg^{-1}$) and E is ET ($kg s^{-1} m^{-2}$ or $mm s^{-1}$). The land-surface representation in ALEXI model is based on the series version of the two-source energy balance (TSEB) model of Norman et al. [3], which partitions the composite surface radiometric temperature, T_{RAD} , into

characteristic soil and canopy temperatures, T_s and T_c , based on the local vegetation cover fraction apparent at the thermal sensor view angle, $f(\theta)$:

$$T_{RAD} \approx \{f(\theta)T_c + [1 - f(\theta)]T_s\}, \tag{2}$$

(Fig. 1), where $f(\theta)$ can be related to leaf area index (LAI) using Beer’s law. Eq. 2 is a linear approximation to an aggregation of surface radiance values. With information about T_{RAD} , LAI, and radiative forcing, the TSEB evaluates the soil (subscript ‘s’) and the canopy (‘c’) energy budgets separately, computing system and component fluxes of net radiation ($RN=RN_C+RN_S$), sensible and latent heat ($H=H_C+H_S$ and $\lambda E=\lambda E_C+\lambda E_S$), and soil heat (G). Importantly, because angular effects are incorporated into the decomposition of T_{RAD} , the TSEB can accommodate TIR data acquired at off-nadir viewing angles by geostationary satellites.

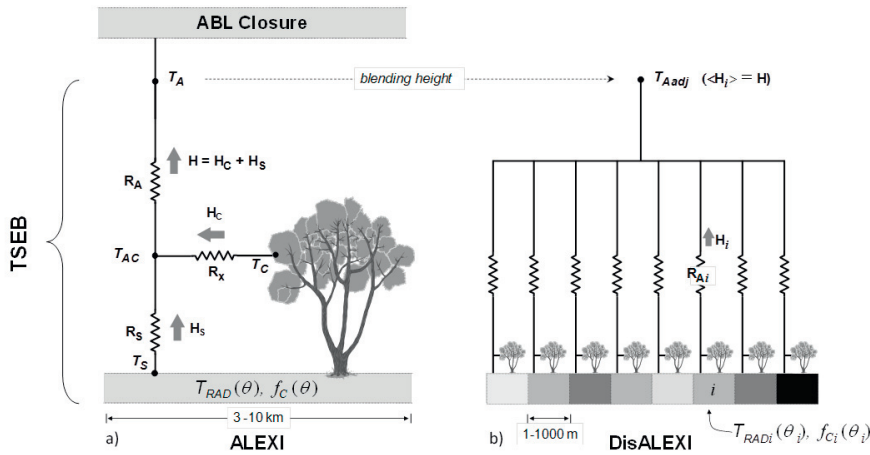


Fig. 1 Schematic diagram representing the coupled ALEXI (a) and DisALEXI (b) modeling scheme, highlighting fluxes of sensible heat (H) from the soil and canopy (subscripts ‘c’ and ‘s’) along gradients in temperature (T), and regulated by transport resistances R_a (aerodynamic), R_x (bulk leaf boundary layer) and R_s (soil surface boundary layer). DisALEXI uses the air temperature diagnosed by ALEXI near the blending height (T_A) to disaggregate 3 to 10-km ALEXI fluxes, given vegetation cover ($f_c(q_i)$) and directional surface radiometric temperature ($T_{RAD}(q_i)$) information derived from high-resolution remote-sensing imagery at look angles q_i . T_A is iteratively adjusted to ensure that DisALEXI H reaggregates on average to the ALEXI-derived H at the coarse ALEXI pixel scale.

The TSEB has a built-in mechanism for detecting thermal signatures of stress in the soil and canopy. An initial iteration assumes the canopy transpiration (λE_C) is occurring a potential (non-moisture limited) rate, while the soil evaporation rate (λE_S) is computed as a residual to the system energy budget. If the vegetation is stressed and transpiring at significantly less than the potential rate, λE_C will be overestimated and the residual λE_S will become negative. Condensation onto the soil is unlikely midday on clear days, and therefore $\lambda E_S < 0$ is considered a signature of system stress. Under such circumstances, the λE_C is iteratively down-regulated until $\lambda E_S \sim 0$ (expected under dry conditions).

For regional-scale applications of the TSEB, the air temperature boundary condition, T_A in Fig. 1, must be specified at the spatial resolution of the geostationary thermal data (typically 3-10 km). Due to localized land-atmosphere feedback, this cannot be accomplished with adequate accuracy using standard synoptic measurements, with typical spacing in the US of 100 km. To overcome this limitation, the TSEB has been coupled with an atmospheric boundary layer (ABL) model, thereby simulating land-atmosphere feedback internally. In the ALEXI model, the TSEB is applied at two times during the

morning ABL growth phase (between sunrise and local noon), using TIR data obtained from a geostationary platform. Energy closure over this interval is provided by a simple slab model of ABL development [4], which relates the rise in air temperature in the mixed layer to the time-integrated influx of sensible heat from the land surface. As a result of this configuration, ALEXI uses only time-differential temperature signals, thereby minimizing flux errors due to absolute sensor calibration and atmospheric and emissivity corrections [5]. The primary radiometric signal is the morning surface temperature rise, while the ABL model component uses only the general slope (lapse rate) of the atmospheric temperature profile [1].

For resolutions requiring higher spatial resolution than that provided by geostationary satellites, the coarse-scale flux estimates from ALEXI can be spatially disaggregated to micrometeorological scales resolving the flux sensor footprint (typically ~100 m) using the DisALEXI technique [6-8]. DisALEXI is a nested modeling approach that uses air temperature diagnosed by ALEXI along with high resolution LAI and LST data from polar orbiting satellites to estimate fluxes at finer scales. The ALEXI air temperature boundary is iteratively refined to conserve H at the ALEXI pixel scale (see Fig. 1).

2.2. Data fusion

Thermal satellite systems are typically characterized by either high spatial resolution (i.e., <100 m) and low temporal resolution (> 16 day revisit – e.g., Landsat) or low spatial resolution (1-10 km) and high temporal resolution (15 minutes to 1 day – e.g., geostationary, MODIS, AVHRR). To effectively track vegetation stress at the field-scale requires monitoring at ~100 m resolution and daily timesteps. This requires either a prognostic modeling approach, or fusion of output generated using multiple diagnostic sensors with differing spatiotemporal characteristics. The ideal solution may be a combination of these approaches, for example using data assimilation techniques.

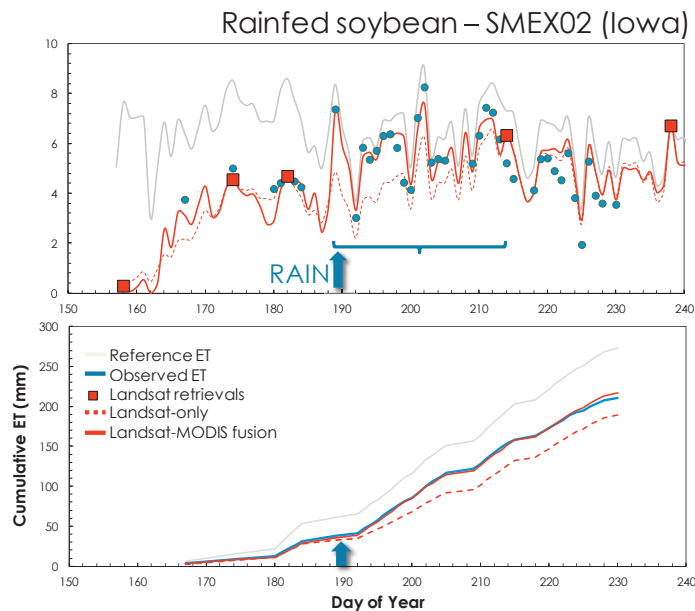


Fig. 2 Comparison of Landsat-only (red dashed lines) and fused Landsat-MODIS (solid red lines) reconstructions of a) daily ET and b) cumulative ET with flux observations (blue dots/line) in a soybean field (site 161) from the SMACEX02 field campaign in central Iowa [9]. Also shown are reference ET (gray lines), and retrieved values on Landsat overpass dates (red boxes).

Cammalleri et al. [9] describe a methodology for combining ALEXI/DisALEXI ET retrievals from geostationary satellites (yielding diurnal information at 10 km), MODIS (daily snapshot assessments at 1 km) and Landsat (providing field scale spatial structure at roughly monthly timesteps). The method uses the Spatial and Temporal Adaptive Reflectance Fusion Model [STARFM: 10]. Cammalleri et al. demonstrated that, on average, the fused retrievals provide better agreement with flux tower data than does a typical Landsat-only temporal interpolation scheme, conserving actual-to-reference ET between clear-sky overpasses [e.g., 8]. The main benefit of incorporating the MODIS scale data is realized when a rainfall event occurs between Landsat overpasses, and when the cover fraction is relatively low with a significant contribution to ET from soil evaporation, as demonstrated in Fig. 2.

3. Evaporative Stress Index

Spatial and temporal variations in instantaneous ET at the continental scale are primarily due to variability in moisture availability (antecedent precipitation), radiative forcing (cloud cover, sun angle), vegetation amount, and local atmospheric conditions such as air temperature, wind speed and vapor pressure deficit. Potential ET describes the evaporation rate expected when soil moisture is non-limiting, ideally capturing response to all other forcing variables. To isolate effects due to spatially varying soil moisture availability, a simple Evaporative Stress Index (ESI) has been developed, describing the departure of model flux estimates of ET from a reference ET rate expected under non-moisture limiting conditions [11,12]. The ESI is computed as standardized temporal anomalies in the ratio of actual to reference ET (AET/refET), and shows good correspondence with standard drought metrics and with patterns of antecedent precipitation, but at significantly higher spatial resolution due to limited reliance on ground observations. This ratio has a value close to 1 when there is ample moisture/no stress, and a value of 0 when ET has been cut off due to stress-induced stomatal closure and/or complete drying of the soil surface. It therefore serves as a valuable proxy indicator for available soil moisture [13-16]. Where there is vegetation, the proxy reflects information over the full rootzone, while it reflects surface moisture conditions (nominally the top 5 cm of soil profile) in areas of very sparse vegetation.

Anderson et al. [17] tested a variety of widely used scaling fluxes in the formulation of the ESI, and found best comparison with precipitation-based metrics and SM anomalies when using the Noah LSM using reference ET using the FAO-96 Penman-Monteith formulation [18]. The ESI is routinely generated over the continental US (CONUS) at 10-km resolution during the growing season, using ALEXI clear-sky ET retrieved shortly before local noon (<http://hrs1.arsusda.gov/drought/>). Temporal composites are generated for 2, 4, 8 and 12-week windows moving at weekly time steps, then anomalies from long-term baseline conditions (currently 2000-2011) for each window are computed, normalized by the standard deviation over the baseline period. The ESI therefore represents sigma values above (wetter) and below (drier) normal conditions in the specified ET ratio for every point in the monitoring domain.

Using high-resolution daily ET datastreams generated using Landsat-MODIS data fusion, as described above, the possibility exists to extend the ESI evaluation down to field scales. This will allow more spatially detailed evaluation of the drought resilience/susceptibility of different crops, grown under different climatic and edaphic conditions.

4. Applications

4.1. Continental scales

Anderson et al. [11,12,17] compared ESI over CONUS with spatiotemporal patterns in other standard drought indices based on precipitation data including the Palmer Drought Severity Index [PDSI: 19],

Standardized Precipitation Index [SPI: 20,21], and ensemble ET and soil moisture percentile products generated with the prognostic North American Land Data Assimilation System (NLDAS) LSM modeling suite [22,23]. In general, good correspondence is observed between anomalies derived from precipitation and ET retrievals, and with patterns in the U.S. Drought Monitor [USDM: 24]. Of these indices, ESI shows best agreement with the NLDAS soil moisture products. Differences in behavior between ALEXI and NLDAS ET are most notable in the Mississippi River basin, where ALEXI predicts significantly lower variability in evaporative flux than do the prognostic LSMs. This would be expected due to localized enhancements in soil moisture from the shallow water table and active irrigation present within the basin. The TIR inputs to ALEXI capture the effects of non-precipitation related moisture inputs without the need for ancillary information about water table or irrigation intensity – a benefit for global applications where such information is not reliably available.

The ESI shows particular capacity for capturing rapid onset drought events, sometimes referred to as „flash droughts“ [25]. Although drought is often thought of as a slowly developing climate phenomenon that can take several months or even years to reach its maximum intensity, drought onset can be very rapid if extreme atmospheric anomalies persist for several weeks. Vegetation health can deteriorate very quickly if moderate precipitation deficits are accompanied by an intense heat wave, strong winds, and sunny skies, as the enhanced ET quickly depletes root zone moisture [26]. The ALEXI energy balance scheme incorporates these important driving variables in its evaluation of ET. Furthermore, LST is a relatively rapid response variable, which reflects increases in soil and canopy temperatures as soil moisture deficits and vegetation stress develop, and in some cases prior to measurable reductions in shortwave vegetation indices [27].

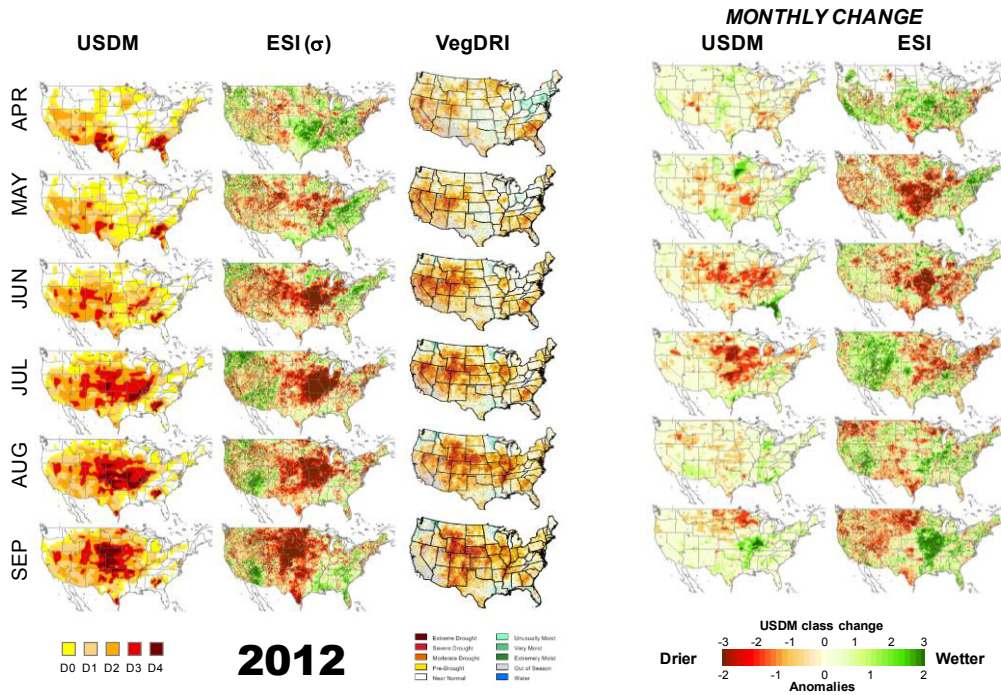


Fig. 3 Monthly maps of USDM drought class, ESI, and VegDRI (left 3 columns). Right columns show change in USDM class and ESI between monthly reports, expressed as normalized anomalies.

The early warning potential of the ESI was demonstrated during the flash drought event that occurred over the central US during 2012, driven by precipitation deficits coupled with a high temperature anomaly. Figure 3 compares evolution of drought classifications recorded in the USDM over the growing season with patterns in the ESI and the Vegetation Drought Response Index [VegDRI: 28], which represents drought signals reflected in anomalies in the Normalized Difference Vegetation Index (NDVI). Changes in USDM class and ESI values over monthly intervals are also shown. The ESI shows signals of stress in what was to become the core of the drought impacted area in May, while significant response in the USDM and VegDRI in this region did not become apparent until July. The differential response between ESI and USDM is also demonstrated in the change indicators mapped in Fig 3. Routine generation of ESI change products could benefit USDM classifications by allowing earlier identification of emerging areas of drought development.

4.2. Field scales

Over heterogeneous landscapes, the 10-km pixels in the CONUS ESI product will often reflect integrated response of multiple land-cover types at different phenological stages – particularly in agricultural regions (see Fig. 4). To facilitate crop condition monitoring and yield estimation, it will be important to disaggregate apparent stress signals down to scales of individual farm fields. At present, only Landsat provides routine, global TIR imagery at this crucial spatial scale (Fig. 4). Fusion of geostationary/MODIS/Landsat ET datastreams may provide valuable temporal information about developing vegetation stress conditions on a field-by-field basis. Timing (i.e. occurrence during the growing season) and duration of moisture deficits determine effects on crop health and consequently the yield, since crop susceptibility to drought varies over the growing season. Even short periods of intense water stress can lead to significant yield loss and reduced grain quality if they occur during sensitive stages in crop development such as emergence, pollination, and grain filling [e.g., 29,30-34].

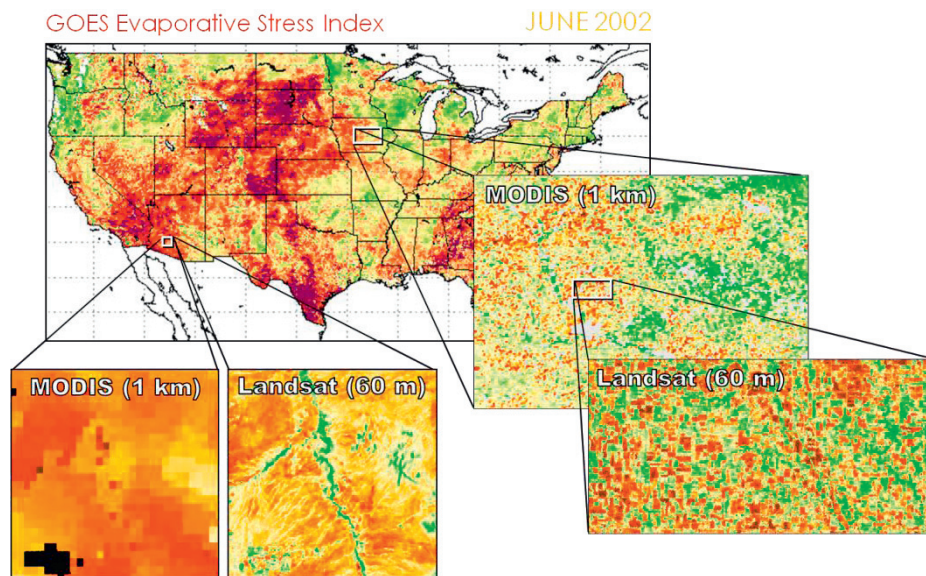


Fig. 4 Example of disaggregation of geostationary satellite-derived ESI using MODIS and Landsat TIR data.

Studies are underway to analyze correlations between spatiotemporal stress information conveyed by the 10-km ESI with monthly county-level crop condition and at-harvest yield datasets collected by the National Agricultural Statistics Service (NASS). We would expect these correlations to improve at spatial resolutions where response of individual crop types can be isolated. Reliable precipitation data at these spatial scales are particularly difficult to obtain, underscoring the value of diagnostic TIR-based monitoring techniques. In other work, we are assessing means to integrate daily AET/refET datastreams from ALEXI/DisALEXI with crop modelling systems like the decision support system for agrotechnology transfer [DSSAT: 35], either through daily reinitialization of model soil moisture variables or through data assimilation techniques. An integrated DSSAT-ESI system would facilitate gridded implementation of crop models in regions with limited availability of soils and precipitation data.

5. Conclusions

A multi-sensor, multi-scale approach to mapping ET and moisture stress using thermal remote sensing data from both geostationary and polar-orbiting satellite platforms has been described. Global implementation of the ALEXI modeling system requires collation and cross-calibration of imagery from multiple geostationary platforms operated by many different countries. Fortunately, archives of global geostationary data are now being constructed to support global monitoring applications. Two projects supporting this effort include the International Satellite Cloud Climatology Project (ISCCP) B1 data rescue project [36] instigated by NOAA, and the Geoland2 project under the European GMES (Global Monitoring for Environment and Security) initiative [37].

For field-scale monitoring, we are limited by the availability and temporal frequency of global high-resolution (100 m) TIR imaging systems. The Landsat Data Continuity Mission (LDCM, or Landsat 8) was successfully launched on 11 February 2013. Landsat 8 will provide high-quality TIR and shortwave data globally with a 16-day revisit, supplementing datasets currently collected by Landsat 7, which have provided incomplete scene coverage due to a scan-line corrector failure since 2003. However, LDCM has a design life of 5 years, and currently there is no funding in place in the U.S. for construction and launch of a follow-on mission. International cooperation in developing a constellation of similar TIR imaging missions would help to avoid gaps in global TIR coverage and water use estimates at the critical field spatial scale, and to significantly improve temporal sampling.

Acknowledgements

This work was supported by NOAA/CTB Grant GC09-236, NASA grant NNH11AQ82I, and by Vaadia-BARD Postdoctoral Fellowship Award No. FI-421-2009 from BARD, the United States - Israel Binational Agricultural Research and Development Fund. USDA is an equal opportunity provider and employer.

References

- [1] Anderson MC, Norman JM, Diak GR, Kustas WP, Mecikalski JR. A two-source time-integrated model for estimating surface fluxes using thermal infrared remote sensing. *Remote Sens. Environ.* 1997;**60**:195-216.
- [2] Anderson MC, Norman JM, Mecikalski JR, Otkin JA, Kustas WP. A climatological study of evapotranspiration and moisture stress across the continental U.S. based on thermal remote sensing: I. Model formulation. *J. Geophys. Res.* 2007;**112**, D10117, doi:10.11029/12006JD007506.

- [3] Norman JM, Kustas WP, Humes KS. A two-source approach for estimating soil and vegetation energy fluxes from observations of directional radiometric surface temperature. *Agric. For. Meteorol.* 1995;**77**:263-293.
- [4] McNaughton KG, Spriggs TW. A mixed-layer model for regional evaporation. *Boundary-Layer Meteorol.* 1986;**74**:262-288.
- [5] Kustas WP, Diak GR, Norman JM. Time difference methods for monitoring regional scale heat fluxes with remote sensing. *Land Surface Hydrology, Meteorology, and Climate: Observations and Modeling* 2001;**3**:15-29.
- [6] Norman JM, Anderson MC, Kustas WP, French AN, Mecikalski JR, Torn RD, Diak GR, Schmugge TJ, Tanner BCW. Remote sensing of surface energy fluxes at 10¹-m pixel resolutions. *Water Resour. Res.* 2003;**39**: doi:10.1029/2002WR001775.
- [7] Anderson MC, Norman JM, Mecikalski JR, Torn RD, Kustas WP, Basara JB. A multi-scale remote sensing model for disaggregating regional fluxes to micrometeorological scales. *J. Hydrometeorol.* 2004;**5**:343-363.
- [8] Anderson MC, Kustas WP, Alfieri JG, Hain CR, Prueger JH, Evett SR, Colaizzi PD, Howell TA, Chavez JL. Mapping daily evapotranspiration at Landsat spatial scales during the BEAREX'08 field campaign. *Adv. Water Resour.* 2012;**50**:162-177.
- [9] Cammalleri C, Anderson MC, Gao F. Fusion of Landsat-MODIS flux fields for mapping daily evapotranspiration at subfield scales. *Water Resources Res.* 2013.
- [10] Gao F, Masek J, Schwaller M, Hall FG. On the blending of the Landsat and MODIS surface reflectance: predicting daily Landsat surface reflectance. *IEE Trans. Geosci. Remote. Sens.* 2006;**44**:2207-2218.
- [11] Anderson MC, Norman JM, Mecikalski JR, Otkin JA, Kustas WP. A climatological study of evapotranspiration and moisture stress across the continental U.S. based on thermal remote sensing: II. Surface moisture climatology. *J. Geophys. Res.* 2007;**112**, D11112, doi:11110.11029/12006JD007507.
- [12] Anderson MC, Hain CR, Wardlow B, Mecikalski JR, Kustas WP. Evaluation of a drought index based on thermal remote sensing of evapotranspiration over the continental U.S. *J. Climate* 2011;**24**:2025-2044.
- [13] Hain CR, Mecikalski JR, Anderson MC. Retrieval of an available water-based soil moisture proxy from thermal infrared remote sensing. Part I: Methodology and validation. *J. Hydrometeorology* 2009;**10**:665-683.
- [14] Hain CR, Crow WT, Anderson MC, Mecikalski JR. An ensemble Kalman filter dual assimilation of thermal-infrared and microwave satellite observations of soil moisture into the Noah land surface model. *Water Resources Res.* 2012;**48**, W11517, doi: 11510.11029/12011WR011268.
- [15] Yilmaz MT, Crow WT, Anderson MC, Hain CR. An objective methodology for merging satellite and model-based soil moisture products. *Water Resources Res.* 2012;**48**, W11502.
- [16] Anderson WB, Zaitchik BF, Hain CR, Anderson MC, Yilmaz MT, Mecikalski JR, Schultz L. Towards an integrated soil moisture drought monitor for East Africa. *Hydrol. Earth Syst. Sci.* 2012;**16**:2893-2913.
- [17] Anderson MC, Hain CR, Otkin JA, Zhan X, Mo KC, Svoboda M, Wardlow B, Pimstein A. An intercomparison of drought indicators based on thermal remote sensing and NLDAS-2 simulations with U.S. Drought Monitor classifications. *J. Hydrometeorology* 2013;
- [18] Allen RG, Pereira LS, Raes D, Smith M. *Crop Evapotranspiration: Guidelines for Computing Crop Water Requirements*. United Nations FAO, Irrigation and Drainage Paper 56. Rome, Italy.1998.
- [19] Palmer WC. Meteorological drought. In Washington, D.C.: U.S. Weather Bureau Research Paper 45; 1965.
- [20] McKee TB, Doesken NJ, Kleist J. The relationship of drought frequency and duration to time scales. In, *AMS Eighth conf. on Applied Climatology*. Anaheim, CA. 1993; p. 179-184.
- [21] McKee TB, Doesken NJ, Kleist J. Drought monitoring with multiple time scales. In, *AMS Ninth conf. on Applied Climatology* Dallas, TX. 1995; p.233-236.
- [22] Xia Y, Mitchell KE, Ek MB, Sheffield J, Cosgrove BA, Wood EF, Luo L, Alonge C, Wei H, Meng J, Livneh B, Lettenmaier DP, Koren V, Duan Q, Mo KC, Fan Y, Mocko D. Continental-scale water and energy flux analysis and validation of the North American Land Data Assimilation System project phase 2 (NLDAS-2): 1. Intercomparison and application of model products. *J. Geophys. Res.* 2012;**117**, doi:10.1029/2011JD016048.
- [23] Xia Y, Ek MB, Wei H, Meng J. Comparative analysis of relationships between NLDAS-2 forcings and model outputs. *Hydrological Processes* 2012;**26**:467-474.
- [24] Svoboda M, LeComte D, Hayes M, Heim R, Gleason K, Angel J, Rippey B, Tinker R, Palecki M, Stooksbury D, Miskus D, Stephens S. The Drought Monitor. *Bull. Amer. Meteorol. Soc.* 2002;**83**:1181-1190.
- [25] Otkin JA, Anderson MC, Hain CR, Mladenova IE, Basara JB, Svoboda M. Examining rapid onset drought development using the thermal infrared based Evaporative Stress Index. *J. Hydrometeorology* 2013.
- [26] Mozny M, Tnka M, Zalud Z, Hlavinka P, Nekova, J, Potop V, Virag M. Use of a soil moisture network for drought monitoring in the Czech Republic. *Theor. Appl. Climatology* 2012;**107**:88-111.
- [27] Moran MS. Thermal infrared measurement as an indicator of plant ecosystem health. In D.A. Quattrochi & J. Luvall (Eds.), *Thermal Remote Sensing in Land Surface Processes*, Taylor and Francis. 2003; p.257-282.
- [28] Brown JF, Wardlow BD, Tadesse T, Hayes MJ, Reed BC. The Vegetation Drought Response Index (VegDRI): a new integrated approach for monitoring drought stress in vegetation. *GIScience and Remote Sensing* 2008;**45**:16-46.

- [29] Barnabás B, Jäger K, Fehér A. The effect of drought and heat stress on reproductive processes in cereals. *Plant, Cell & Environment* 2008;**31**:11-38.
- [30] Rotter R, Geijn VD. Climate change effects on plant growth, crop yield, and livestock. *Climate Change* 1999;**43**:651-681.
- [31] Saini HS, Westgate ME. Reproductive development in grain crops during drought. *Advances in Agronomy* 1999;**68**:59-96.
- [32] Li YP, Ye W, Wang M, Yan XD. Climate change and drought: a risk assessment of crop-yield impacts. *Climate Research* 2009;**39**:31-46.
- [33] Mishra V, Cherkauer K. Retrospective droughts in the crop growing season: Implications to corn and soybean yield in the Midwestern United States. *Agricultural and Forest Meteorol.* 2010;**150**:1030-1045.
- [34] Pradhan GP, Prasad PV, Fritz AK, Kirkham MB, Gill BS. Response of Aegilops species to drought stress during reproductive stages of development. *Functional Plant Biology* 2012;**39**:51-59.
- [35] Jones JW, Hoogenboom G, Porter CH, Boote KJ, Batchelor WD, Hunt LA, Wilkens PW, Singh U, Gijsman AJ, Ritchie JT. The DSSAT cropping system model. *Eur. J. Agron.* 2003;**18**:235-265.
- [36] Knapp KR. Scientific data stewardship of International Satellite Cloud Climatology Project B1 geostationary observations. *J. Appl. Remote Sensing* 2008;**2**:023548, doi:10.1117/1.3043461
- [37] Lacaze R, Balsamo G, Baret F, Bradley A, Calvet JC, Camacho F, D'Andrimont R, Freitas SC, Makhmara H, Naeimi V, Pacholczyk P, Poilvé H, Smets B, Tansey K, Trigo IF, Wagner W, Weiss M. Geoland2 - Towards an operational GMES land monitoring core service; First results of the biogeophysical parameter core mapping service. In W. Wagner & B. Székely (Eds.), *ISPRS TC VII Symposium – 100 Years ISPRS* Vienna, Austria,: ISPRS. 2010; p.354-359.